© 1999 The Chemical Society of Japan

Syntheses, Structures, and Redox Properties of 1,4-Bis(dimesitylphosphino)-2,3,5,6-tetrafluorobenzene and the Corresponding Bis(phosphoryl) and Bis(phosphonio) Derivatives

Shigeru Sasaki, Yoshihiro Tanabe, and Masaaki Yoshifuji*

Department of Chemistry, Graduate School of Science, Tohoku University, Aramaki-Aoba, Sendai 980-8578

(Received October 12, 1998)

Sterically hindered 1,4-bis(dimesitylphosphino)-2,3,5,6-tetrafluorobenzene (**1**) was synthesized by the aromatic nucleophilic substitution of lithium dimesitylphosphide with hexafluorobenzene. Two phosphorus atoms of **1** were oxidized and methylated to give the corresponding bis(phosphoryl)benzene **2** and bis(phosphonio)benzene $\mathbf{3}^{2+}\cdot 2\mathrm{TfO}^-$ (TfO^- = trifluoromethanesulfonyl), respectively. On the other hand, reaction of **1** with butyllithium and phenyllithium gave more crowded 2,5-dibutyl-1,4-bis(dimesitylphosphino)-3,6-difluorobenzene (**4**) and 1,4-bis(dimesitylphosphino)-2,5-difluoro-3,6-diphenylbenzene (**5**), respectively. Structures of **1**, **2**, $\mathbf{3}^{2+}\cdot 2\mathrm{TfO}^-$, **4**, and **5** were confirmed by conventional spectroscopic methods; particularly ^{19}F NMR spectroscopy reflected their crowded structures. Molecular structures of **1**, **2**, and $\mathbf{3}^{2+}\cdot 2\mathrm{TfO}^-$, were further investigated by X-ray crystallography, where unusually large bond angles around phosphorus atoms were observed. Electrochemical measurements were carried out to investigate redox properties of **1**, $\mathbf{3}^{2+}\cdot 2\mathrm{TfO}^-$, **4**, and **5**. Although the cyclic voltammogram of diphosphine **1** showed irreversible oxidation waves above 0.8 V, in spite of substitution at all the *ortho* positions to the phosphorus atoms in **1**, displacement of the two fluorine atoms of **1** by the butyl or the phenyl groups lowered the oxidation potential and improved the stability of the corresponding radical cations. Particularly, **5** clearly showed two-step oxidation waves. On the other hand, bis(phosphonium salt) $\mathbf{3}^{2+}\cdot 2\mathrm{TfO}^-$ showed two steps of quasi-reversible redox waves, which suggested reduction to the cation radical and the neutral species, although their stability was limited.

Substitution of electron-donating or withdrawing groups at the 1,4-positions of an aromatic ring is one of the common ways of construction of multi-step redox systems. Although phosphines and phosphonium salts could be regarded as moderate donors and acceptors, respectively, they have rarely been used as substituents for stabilizing π-conjugated redox systems as compared with the second-row elements, because the oxidized form of phosphines and the reduced form of phosphonium salts are usually unstable and reactive. In the course of our investigation on the phosphorus-based functional molecules,[1] we became interested in the sterically hindered phosphines, since all-*ortho*-methylated triarylphosphines, such as trimesitylphosphine,[2] possess unusual structures as well as redox properties: e.g. trimesitylphosphine has extremely large C–P–C angles (109.7°, average[3]), as compared with triphenylphosphine (103.0°),[4] and gives a reversible redox system with an extremely low oxidation potential ($E_{1/2}$ = 0.784 and E_{ox} = 1.400 V vs. SCE for trimesitylphosphine and triphenylphosphine, respectively) affording a stable radical cation.[5] Thus, the sterically hindered phosphine units can be employed as reversible redox-sites of the novel π-conjugated system in a way analogous to the amino groups in *para*-phenylenediamines[6] (Scheme 1). Furthermore, we expected that the sterically hindered *para*-phenylenediphosphines would be converted to novel acceptors by the derivatization to the corresponding bis(phosphonium salt) (Scheme 1). Recently, Weiss et al. synthesized bis(ammonium salt) and bis(phosphonium salt) by the reaction of tertiary amine or phosphine with hexafluorobenzene in the presence of trimethylsilyl triflate.[7] These salts are reported to be moderate electron acceptors displaying quasi-reversible two-step redox waves in cyclic voltammetry.

In this article, we report on the syntheses, structures, and redox properties of 1,4-bis(dimesitylphosphino)-2,3,5,6-tetrafluorobenzene (**1**), 2,5-dibutyl-1,4-bis(dimesitylphosphino)-3,6-difluorobenzene (**4**), 1,4-bis(dimesitylphosphino)-2,5-difluoro-3,6-diphenylbenzene (**5**), 1,4-bis(dimesitylphosphoryl)-2,3,5,6-tetrafluorobenzene (**2**), and 1,4-bis[(dimesityl)methylphosphonio]-2,3,5,6-tetrafluorobenzene bis(trifluoromethanesulfonate) ($\mathbf{3}^{2+}\cdot 2\mathrm{TfO}^-$) (Scheme 2). Diphosphine **1**, an all-*ortho*-substituted *para*-phenylenediphosphine, was synthesized as one of the model compounds of the two-step redox system shown in Scheme 1(a) as well as a synthetic intermediate, although it had four fluorine atoms unfavorable to donor ability for some synthetic reasons. The two fluorine atoms of the four in **1** were further displaced by alkyl or aryl groups to obtain more crowded phosphines as well as to remove any inductive effect of the fluorine atoms. On the other hand, bis(phosphonium salt) $\mathbf{3}^{2+}$ was expected as a two-step redox acceptor. ^{1}H, ^{31}P, and ^{19}F NMR spectra of **2**, $\mathbf{3}^{2+}$, **4** and **5**, particularly ^{19}F NMR spectrum, reflected the sterically crowded structure and the dynamic processes were investigated in terms of variable temperature measurement. The molecular structures of

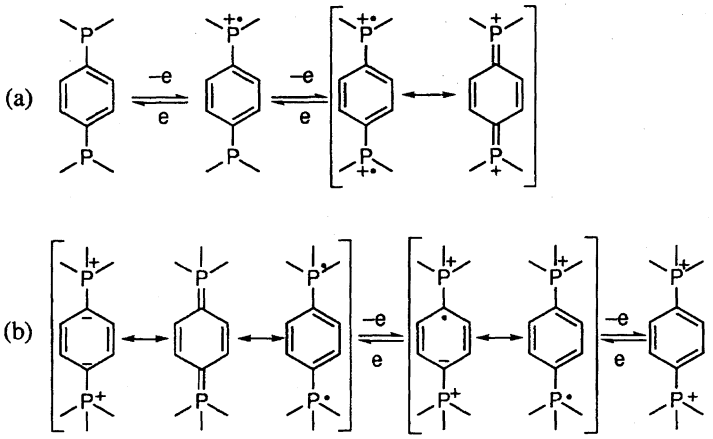

Scheme 1. Redox systems composed of diphosphine and bis(phosphonium salt).

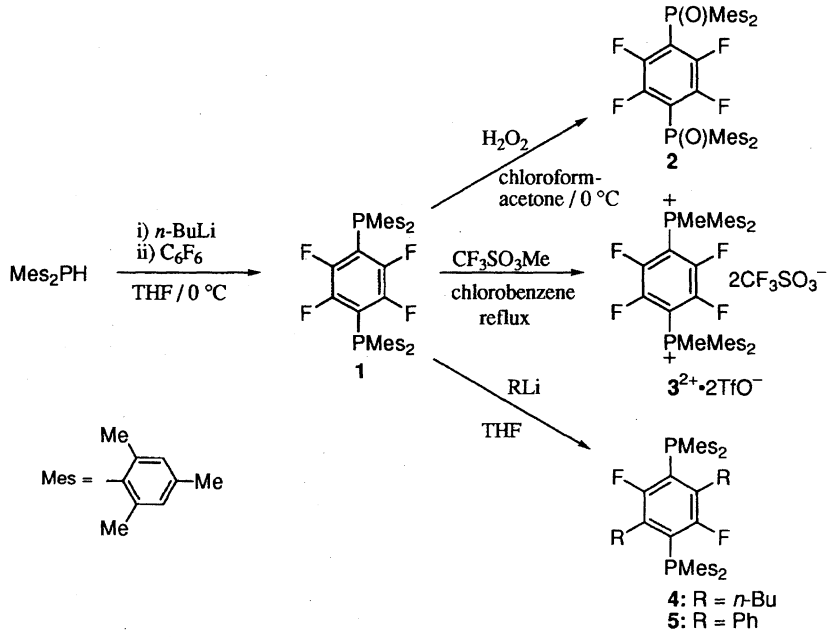

Scheme 2. Synthetic scheme for compounds **2**—**5** from **1**.

1, **2**, and 3^{2+} were further analyzed crystallographically and compared with each other.

Results and Discussion

Synthesis. As representative synthetic routes to *para*-phenylenediphosphines, the following reactions are known: the reactions of aryllithium or the Grignard reagents[8] with phosphorus chlorides, the transition metal catalyzed cross coupling between aryl halides and phosphides,[9] and the aromatic nucleophilic substitution reactions of alkaline-metal phosphide with fluorobenzenes.[10] However, the reaction of the sterically hindered aryllithium or the Grignard reagents with phosphorus chlorides affords triarylphosphines under limited conditions and sometimes a side reaction takes place to afford a tetraaryldiphosphine as a major product.[1] In many cases, the transition-metal catalyzed cross coupling-reaction is not applicable to the sterically hindered systems, while the aromatic nucleophilic substitution proceeds even at the sterically crowded positions. McFarlane and McFarlane reported the introduction of four consecutive diphenylphosphino groups at 1,2,3,4-positions of a benzene ring by the substitution reaction of 1,2,3,4-tetrafluorobenzene with sodium diphenylphosphide.[10] At first, we also employed the reaction of a lithium phosphide with hexafluorobenzene to synthesize poly(phosphino)benzenes, but the reaction of lithium dimesitylphosphide[11] with hexafluorobenzene (0.5 molar amount) in THF afforded diphosphine **1** as an exclusive product (Scheme 2). Substitution at the *ortho* or *meta* position would not be favorable probably due to steric reasons, as the phenomenon has been reported for the other nucleophiles.[12] Under these reaction conditions, dimesityl(pentafluorophenyl)phosphine was not detected at all, in spite of the expected higher reactivity of hexafluorobenzene than dimesityl(pentafluorophenyl)phosphine, probably due to the very fast next reaction of the phosphide with the pentafluorobenzene as an intermediate. Further substitution was not observed even if less amount of hexafluorobenzene (0.33 molar amount) or diphosphine **1** was employed.

On the other hand, the reaction of diphosphine **1** with six molar amounts of methyllithium, butyllithium, or phenyllithium afforded further substituted products (Scheme 2). Although the reaction with methyllithium gave a complex mixture of mono- and dimethylated products, two butyl and phenyl groups were regio-selectively introduced to give diphosphines **4** and **5**, respectively. Addition of mesityllithium to **1** resulted in formation of an inseparable mixture and incorporation of only one mesityl group was confirmed by mass spectroscopy. Reaction of the phosphide with hexachlorobenzene in place of hexafluorobenzene afforded *P*,*P*,*P*′,*P*′-tetramesityldiphosphine[1,2] ($\delta_P = -29.4$) as a major product without formation of substituted products.

The oxidation of **1** by aqueous hydrogen peroxide in acetone–chloroform, followed by recrystallization from dichloromethane–ethanol, afforded bis(phosphine oxide) **2** including two molecules of ethanol in moderate yield (Scheme 2). Although the reaction of **1** with iodomethane or trimethyloxonium tetrafluoroborate gave the desired **3**, isolation of **3** resulted in failure, due to contamination by unknown by-products. Diphosphine **1** was successfully methylated by methyl trifluoromethanesulfonate in chlorobenzene and recrystallization from acetone–hexane gave crystals of bis(phosphonium salt) **3** suitable for X-ray crystallography.

The newly synthesized compounds **1**, **2**, $\mathbf{3}^{2+}\cdot 2TfO^-$, **4**, and **5** are stable and can be handled under air after purification.

Structure and Redox Properties. The structure of diphosphine **1** was easily confirmed by ^1H, ^{13}C, ^{19}F, and ^{31}P NMR spectra, and its mass spectrum. ^{31}P and ^{19}F NMR signals appeared at $\delta = -46.3$ as a broad triplet and $\delta = -131.5$ as a doublet of multiplet, respectively (Fig. 1). Both signals were interpreted as the AA′XX′X″X‴ pattern with $^3J_{PF} = 34$ Hz and $^3J_{FF} = 10$ Hz, which are within the range of known coupling constants of tris(perfluoroaryl)phosphines.[10,13] The molecular structure of diphosphine **1** was further investigated by X-ray crystallography (Table 1 and Fig. 2). Phosphine **1** has C_2 axis at the center of the C_6F_4 ring. The average C–P–C angle (106.8°) of **1** is almost the mean value of those of trimesitylphosphine and triphenylphosphine,[3] although due to the large angle between C4–P1–C13 (113.2(1)°) and the small angle between C1–P1–C13 (100.7(1)°). The phosphorus atoms are located slightly out of the least-squares plane of the C_6F_4 ring (0.306 Å).

Table 1. Selected Bond Lengths, Angles, and Torsion Angles of **1**

	Bond lengths/Å		
P1–C1	1.847(3)	P1–C4	1.833(3)
P1–C13	1.853(3)		
	Bond angles/°		
C1–P1–C4	100.7(1)	C4–P1–C13	113.2(1)
C1–P1–C13	106.6(1)		
	Torsion angles/°		
C2–C1–P1–C4	−74.8(2)	C2–C1–P1–C13	166.8(2)

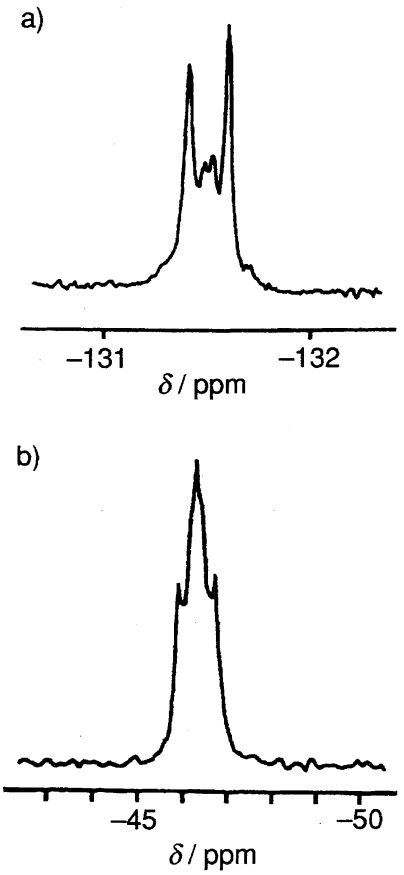

Fig. 1. a) ^{19}F and b) ^{31}P NMR spectra of **1** in $CDCl_3$ at 293 K.

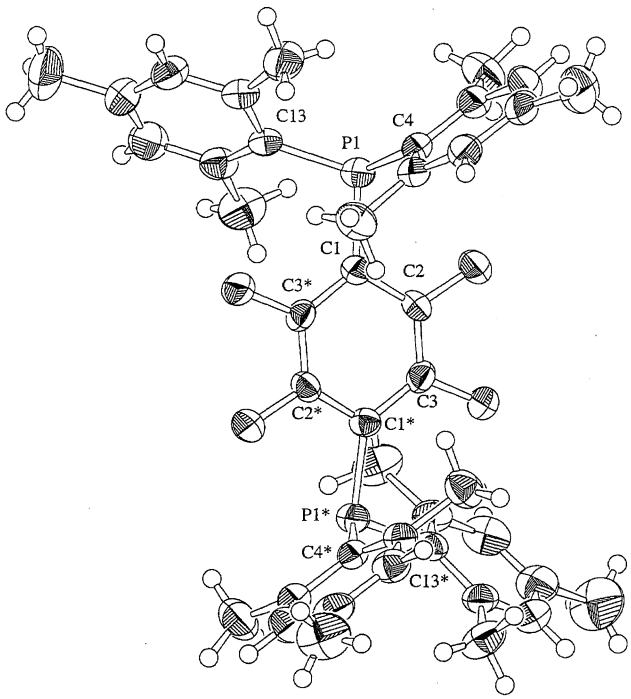

Fig. 2. An ORTEP drawing of molecular structure of **1** with 50% probability ellipsoids.

Diphosphines **4** and **5** displayed more complicated ^{19}F and ^{31}P NMR spectra resulting from the more crowded structure (Fig. 3). ^{19}F and ^{31}P NMR spectra were reproducible by assigning $\delta_P = -43.73, -43.83$, $\delta_F = -104.38, -104.43$, $^3J_{PF} = {}^4J_{PF} = 19$ Hz for **4** and $\delta_P = -38.69, -38.79$, $\delta_F = -100.05, -100.10$, $^3J_{PF} = {}^4J_{PF} = 20$ Hz for **5**. The slightly different chemical shifts of two ^{19}F and ^{31}P nuclei are indicative of the frozen conformation of **4** and **5**, where the environments around two ^{19}F and ^{31}P nuclei are slightly different. Furthermore, the fact that the $^3J_{PF}$ value is smaller than that of **1** suggests that the lone pairs of the phosphorus atoms lie in the direction opposite to the *ortho* F atom.[10] Unusually large $^4J_{PF}$ would be due to the frozen conformation, where ^{19}F and ^{31}P nuclei have a strong interaction through space and/or through four bonds. However, we could not go into further detail because ^{19}F and ^{31}P NMR spectroscopic studies of **4** and **5** did not show sharp differences even at 333 K, where the spectra became only broader and less resolved.

As compared with diphosphine **1**, ^1H, ^{13}C, ^{19}F, and ^{31}P NMR spectra of bis(phosphine oxide) **2** were also more complicated due to the more crowded structure around the phosphorus atoms (Fig. 4). At 293 K, ^{19}F and ^{31}P NMR spectra of **2** in $CDCl_3$ consisted of two broad singlets at $\delta = -129.0, -129.8$ and a singlet at $\delta = 21.8$, respectively. On the other hand, *ortho* and *para* methyl groups of the mesityl groups appeared at the same position in its ^1H NMR spectrum. In order to disclose the dynamic behavior of **2**, variable temperature ^1H, ^{19}F, and ^{31}P NMR measurements were carried out in the temperature range of 220 to 333 K. Although ^{31}P NMR spectrum did not show any significant change and the ^1H NMR spectrum of *ortho* and *para* methyl groups, which appeared as one singlet at the same position ($\delta = 2.27$) at 273 K, became slightly resolved to two singlets ($\delta = 2.24$ and 2.27) at 220 K, the ^{19}F NMR spectrum of **2** showed clear temperature-dependent behavior in the temperature range of 220 to 333 K (Fig. 4). At 220 K, the ^{19}F NMR spectrum of **2** consisted of two sets of the AB pattern with large and small coupling constants ($\delta = -128.3$ and -130.7, $J = 27.0$ Hz and $\delta = -129.2$ and -130.5, $J = 7.68$ Hz, respectively). They became two broad singlets at 270 K and finally coalesced to one singlet ($\delta = -129.4$) at 333 K. We assume that there are four equilibrated stereoisomers, which originate from the directions of oxygen atoms, to interpret this dynamic behavior (Scheme 3). An *ortho* fluorine atom close to oxygen would appear at a higher field and that of the opposite side at a lower field due to the deshielding effect of aromatic rings. At 220 K, their interconversion is slow on the NMR time scale and two sets of molecules were observed. The signal of the major isomer ($\delta = -128.3$ and -130.7, $J = 27.0$ Hz), which has a characteristic large coupling constant between *ortho* fluorine atoms,[13,14] was assigned to **2a**

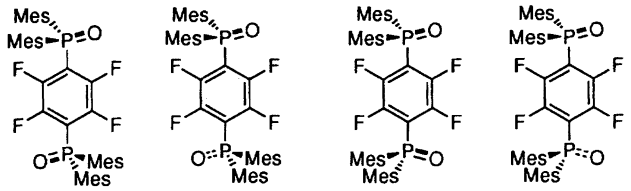

Scheme 3. Conformation of **2**.

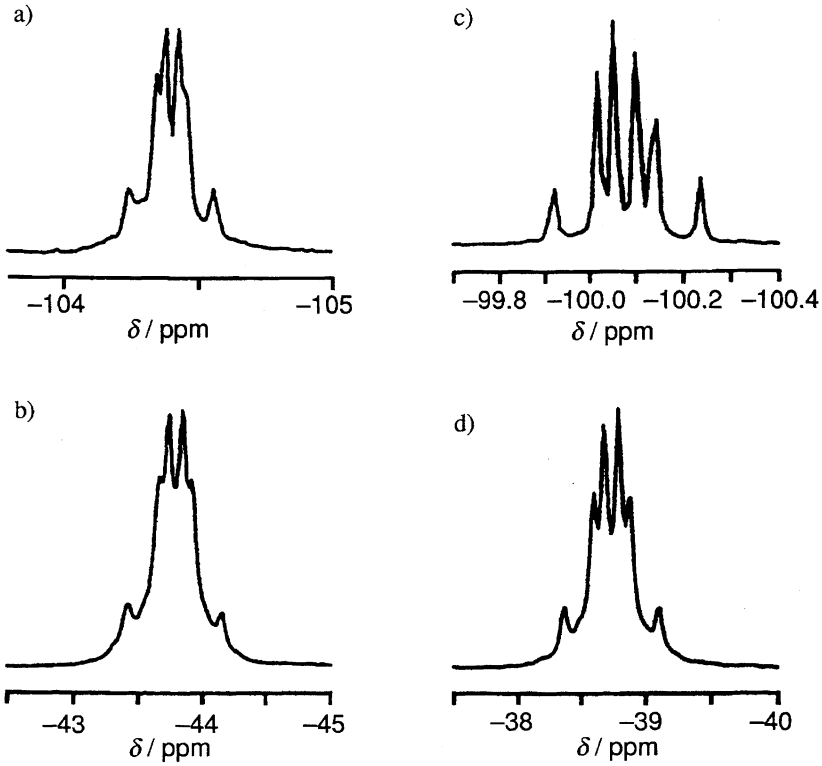

Fig. 3. a) ^{19}F, b) ^{31}P NMR spectra of **4**, c) ^{19}F, d) ^{31}P NMR spectra of **5** in $CDCl_3$ at 293 K.

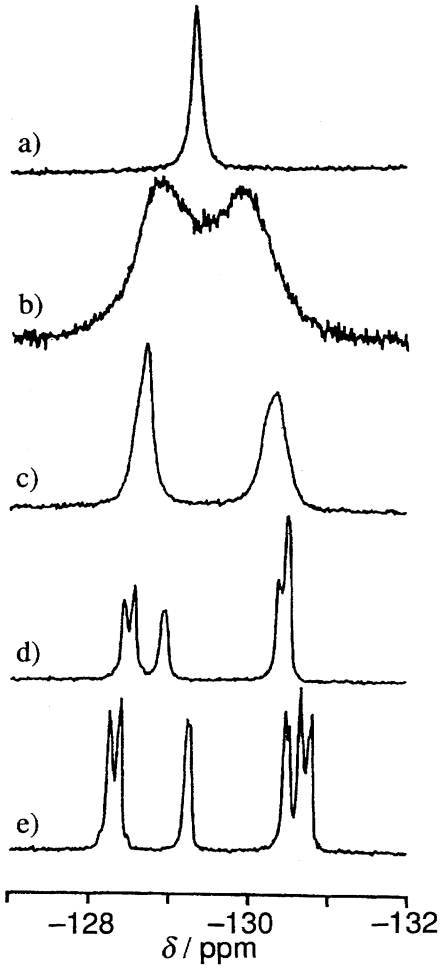

Fig. 4. ^{19}F NMR spectra of **2** in $CDCl_3$ at a) 333 K, b) 293 K, c) 270 K, d) 252 K, and e) 220 K.

and/or **2b**. On the other hand, the remainder was assigned to **2c** and/or **2d** due to lack of the large coupling between ^{19}F nuclei. At higher temperatures, the faster exchange between these isomers resulted in the coalescence and finally **2** was observed as a single isomer. Although the dynamic behavior and diastereomer formation due to the sterically hindered propellers of trimesitylphosphine ligands were reported by Schmidbaur et al.,[15] we could not observe such a dynamic process probably because the van der Waals radius of fluorine atom is smaller than that of the methyl group (1.35 and 2.00 Å respectively). The molecular structure of **2** was investigated by X-ray crystallography of a single crystal including two molecules of ethanol obtained by recrystallization from dichlormethane–ethanol (Fig. 5 and Table 2). Bis(phosphine oxide) **2** has an inversion center on the central aromatic ring. An average C(arom.)–P–C(arom.) bond angle (108.6°) was larger than that of **1** by 1.8° and slightly larger than those known for the free triphenylphosphine oxide (e.g. 106.55°,[16c] 107.1°[16a]) and hydrogen bonded triphenylphosphine oxide (e.g. 107.26°,[17b] 107.4°[17a]), although the difference between the largest C4–P1–C13 (115.7(2)°) and the smallest C1–P1–C13 (101.5(2)°) angles was large. On the other hand, an average C(arom.)–P–O angle (110.1°)

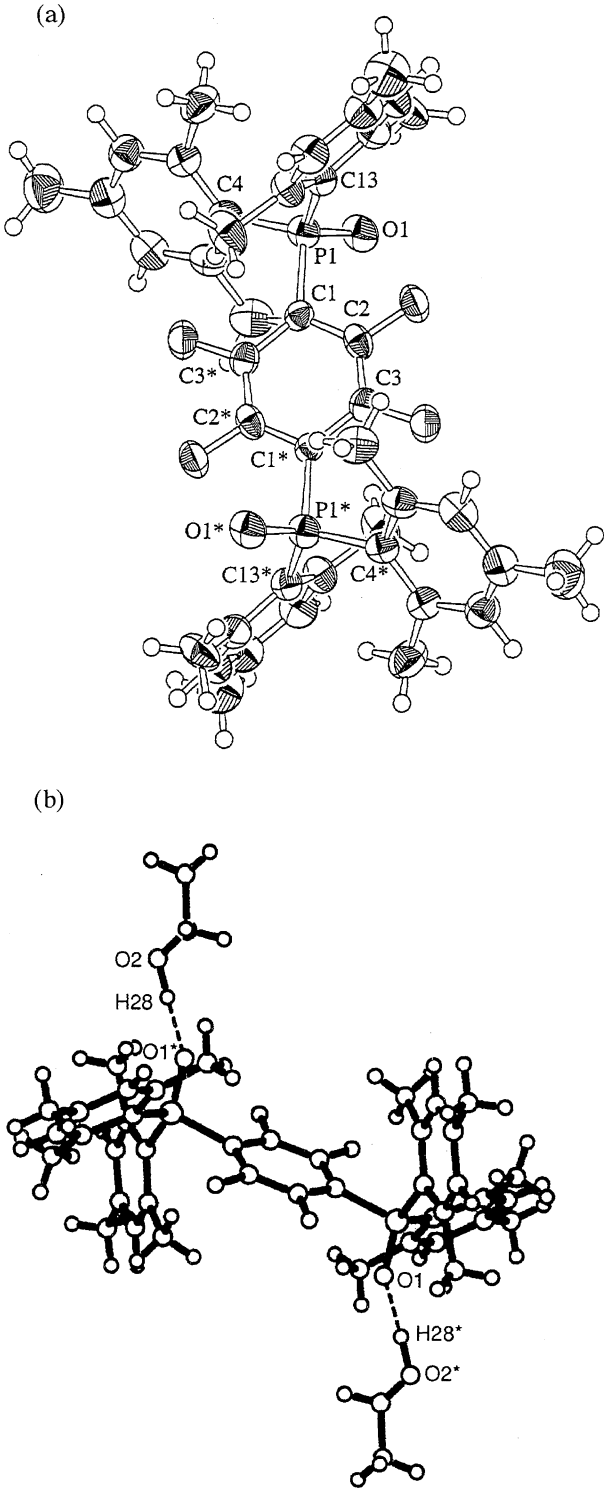

Fig. 5. a) An ORTEP drawing of molecular structure of **2** with 50% probability ellipsoids. b) The hydrogen bonding of **2** with EtOH in the crystal.

became smaller than those of free triphenylphosphine oxide (e.g. 111.7°,[16a] 112.25°[16c]) and the hydrogen bonded triphenylphosphine oxide (e.g. 111.46°,[17a] 111.6°[17b]). A tetrahedral geometry was distorted by the bulky mesityl groups. A dimesitylphosphoryl moiety has a staggered

Table 2. Selected Bond Lengths, Angles, and Torsion Angles of **2**·2EtOH

	Bond lengths/Å		
P1–C1	1.842(5)	P1–C4	1.810(5)
P1–C13	1.824(5)	P1–O1	1.487(3)
O1···O2*	2.683(6)		
	Bond angles/°		
C1–P1–C4	108.6(2)	C4–P1–C13	115.7(2)
C1–P1–C13	101.5(2)	O1–P1–C1	106.3(2)
O1–P1–C4	110.8(2)	O1–P1–C13	113.1(2)
	Torsion angles/°		
C2–C1–P1–C4	169.0(4)	C2–C1–P1–C13	−68.7(4)
O1–P1–C1–C2	49.7(4)		

conformation relative to the central benzene ring with the O1–P1–C1–C2 torsion angle of 49.7(4)°. Two oxygen atoms of the dimesitylphosphoryl moieties point to opposite directions as a result of centrosymmetrical structure, and thus the dipole moment of **2** was canceled. The structure of **2** in crystal coincides with **2b** in Scheme 3 and **2b** might be one of the stereoisomers of the largest population at low temperature. Two ethanol molecules included in the crystal were weakly hydrogen-bonded to the oxygen atoms of phosphine oxides (Fig. 5b), where the hydrogen atom H28 are estimated to locate with O2–H28, O1*···H28, and O2–H28···O1* distances of 1.033 Å, 1.651 Å, and 177.58°, respectively. The incorporation of two molecules of ethanol was further confirmed by ^{1}H and ^{13}C NMR spectra, elemental analysis, and IR spectrum, where the OH stretching at 3421 cm^{-1} was observed in the IR spectrum. Phosphine oxides are good hydrogen acceptors and have been reported to form large mixed crystals with alcohols, amides, amines, and so on.[18] The P1–O1 bond length (1.484(1) Å) was longer than that for the free triphenylphosphine oxide (e.g. 1.46(1),[16a] 1.484(1)[16c] Å) and falls into the shortest category of those reported for hydrogen-bonded triphenylphosphine oxides (e.g. 1.482(4),[17b] 1.493(3)[17a] Å). Relatively shorter P1–O1 bond lengths and longer O1···O2* distances (2.683(6) Å, as compared with known hydrogen-bonded triphenylphosphine oxides (e.g. 2.504(3),[17a] 2.672(5)[17b] Å), suggest a weak hydrogen bond in **2**·2EtOH, which is consistent with OH stretching band at high wave numbers. The reduced basicity due to the inductive effect of a fluorinated aromatic ring would be responsible for it.

Bis(phosphonium) salt $\mathbf{3}^{2+}\cdot 2\mathrm{TfO}^{-}$ showed NMR spectra which appeared to result from rather crowded structure, as compared with that of **2**. Although ^{31}P NMR spectrum consisted of a single peak at δ = 7.2, ^{19}F NMR spectrum (Fig. 6), which was composed of two multiplets and two singlets, disclosed that there are at least two stable isomers of $\mathbf{3}^{2+}\cdot 2\mathrm{TfO}^{-}$ at room temperature. Bis(phosphonium) salt $\mathbf{3}^{2+}\cdot 2\mathrm{TfO}^{-}$ was observed as a single species in ^{1}H NMR spectrum (200 MHz); however, the methyl groups attached to the phosphorus atom were observed as two sets of doublets with slightly different chemical shifts (δ = 3.12, d, J = 12.8 Hz and δ = 3.16, d, J = 12.5 Hz) in ^{1}H NMR spectrum (600 MHz). That observation was consistent with the ^{19}F NMR measurement. No dynamic behavior was observed up to 333 K in ^{1}H, ^{19}F, and ^{31}P NMR measurements.

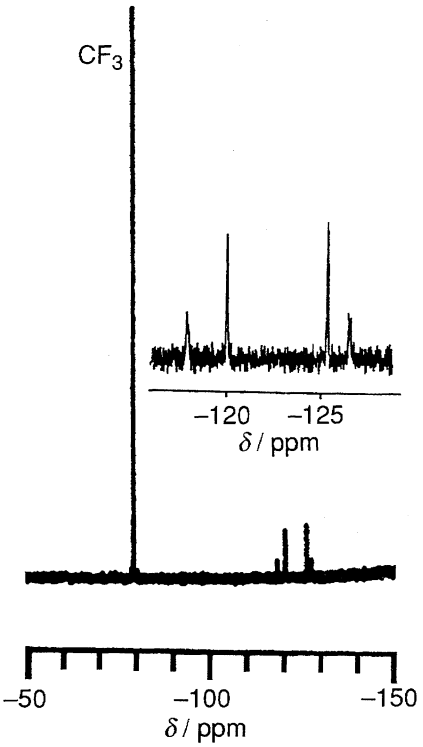

Fig. 6. ^{19}F NMR spectrum of $\mathbf{3}^{2+}\cdot 2\mathrm{TfO}^{-}$ in $CDCl_3$ at 293 K.

Although the NMR spectra did not support formation of $\mathbf{3}^{2+}\cdot 2\mathrm{TfO}^{-}$ clearly, the structure of $\mathbf{3}^{2+}\cdot 2\mathrm{TfO}^{-}$ was confirmed by X-ray crystallography (Fig. 7 and Table 3). In the crystals, two (dimesityl)methylphosphonio groups of $\mathbf{3}^{2+}\cdot 2\mathrm{TfO}^{-}$, separated by the intervening 2,3,5,6-tetrafluoro-1,4-phenylene moiety, had eclipsed conformation. Each (dimesityl)methylphosphonio group took a stag-

Table 3. Selected Bond Lengths, Angles, and Torsion Angles of $\mathbf{3}^{2+}\cdot 2\mathrm{TfO}^{-}$

	Bond lengths/Å		
P1–C1	1.798(7)	P1–C3	1.849(7)
P1–C9	1.815(7)	P1–C18	1.816(7)
P2–C2	1.803(7)	P2–C6	1.834(7)
P2–C27	1.813(6)	P2–C36	1.823(7)
	Bond angles/°		
C3–P1–C9	107.8(3)	C9–P1–C18	110.6(3)
C3–P1–C18	114.4(3)	C1–P1–C3	104.0(3)
C1–P1–C9	115.7(3)	C1–P1–C18	104.4(3)
C6–P2–C27	108.9(3)	C6–P2–C36	112.6(3)
C27–P2–C36	113.2(3)	C2–P2–C6	103.1(3)
C2–P2–C27	113.2(3)	C2–P2–C36	105.4(3)
	Torsion angles/°		
C4–C3–P1–C9	18.2(7)	C4–C3–P1–C18	−105.3(6)
C1–P1–C3–C4	141.5(6)	C5–C6–P2–C27	−8.6(7)
C5–C6–P2–C36	117.8(6)	C2–P2–C6–C5	−129.1(6)

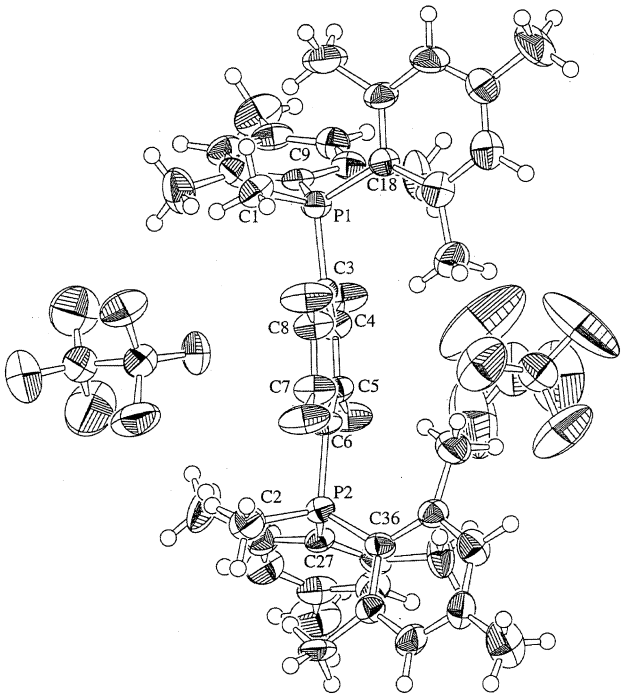

Fig. 7. An ORTEP drawing of the molecular structure of $3^{2+}\cdot 2TfO^{-}$ with 50% probability ellipsoids.

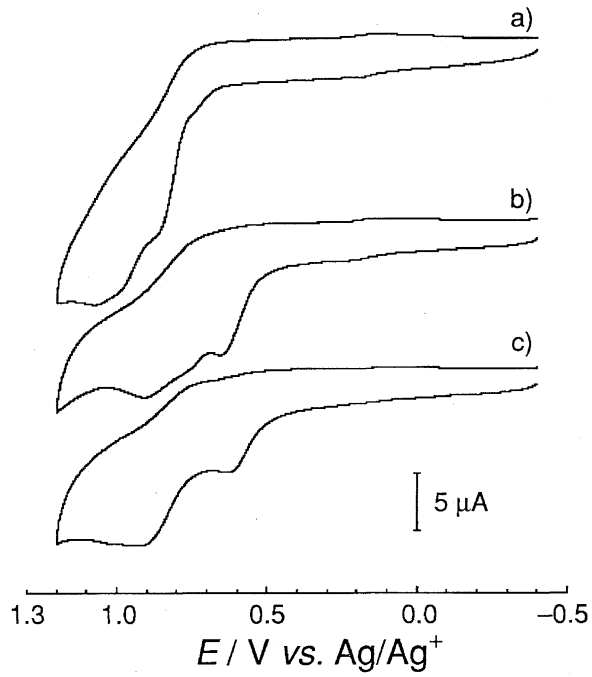

Fig. 8. Cyclic voltammograms of a) **1**, b) **4**, and c) **5** in dichloromethane. Scan rate: 60 mV s^{-1}.

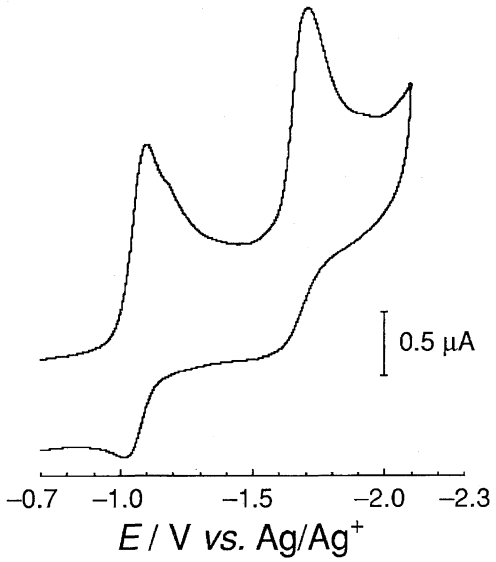

Fig. 9. Cyclic voltammograms of $3^{2+}\cdot 2TfO^{-}$ in benzonitrile. Scan rate: 10 mV s^{-1}.

gered conformation against the central benzene ring with the C1–P1–C3–C4 and C2–P2–C6–C5 torsion angles as 141.5(6) and −129.1(6)°, respectively. Phosphorus atoms had a tetrahedral configuration where the C(arom.)–P–C(arom.) angles range from 107.8(3) to 114.4(3)° with the average value as 110.9 and 111.6° for P1 and P2, respectively, which are larger than those for **1** and **2**, in spite of the attachment of the relatively large methyl group. On the other hand, the C(Me)–P–C(arom.) angles range from 103.1(3) to 115.7(3)° with the average values of 108.0 and 107.2° for P1 and P2, respectively. The large differences of each bond angle around phosphorus atoms are characteristic of this sterically hindered molecule, as compared with methyltriphenylphosphonium,[19] which has an almost complete tetrahedral arrangement without significant deviation. The two trifluoromethanesulfonate groups were placed on both sides of the central aromatic ring without intermolecular short contacts less than the sum of van der Waals radii.

The redox properties of **1**, **4**, **5**, and $3^{2+}\cdot 2TfO^{-}$ were investigated by cyclic voltammetry (Figs. 8 and 9). Diphosphine **1** showed an unresolved irreversible oxidation wave above 0.8 V vs. Ag/Ag^{+} (Fig. 8a). Although both phosphorus atoms of **1** bear three all-*ortho*-substituted aryl groups, oxidation of **1** did not generate a stable radical cation like trimesitylphosphine.[5] The sharp C(central aryl)–P–C(Mes) angles of **1**, as well as the inductive effect of perfluorinated aryl group, would destabilize the radical cation of **1**. As compared with **1**, diphosphines **4** and **5** gave clearer two-step oxidation waves at a lower potential (Figs. 8b and 8c, E_{ox} = 0.66, 0.91 V, ΔE_{ox} = 0.25 V for **4**; E_{ox} = 0.63, 0.92 V, ΔE_{ox} = 0.29 V for **5**). Displacement of the two fluorine atoms by the butyl or phenyl groups and the resulting more crowded environment around the phosphorus atoms might lower the redox potentials and stabilize the radical cations. The first oxidation potentials of **4** and **5** fall into the category of the smallest oxidation potentials as triarylphosphines.[5a] On the other hand, small charge delocalization to the central aromatic ring, due to the small resonance effect resulting from the long phosphorus–carbon bond length which does not allow effective 3p-2p orbital overlap and inherently localized character of triarylphosphine cation radicals, resulted in the small ΔE_{ox} values. Although redox waves were still irreversible in spite of crowded structure around phosphorus atoms, these are the first example of a multistep redox system composed of tri-

arylphosphines, to the best of our knowledge. Bis(phosphonio) derivative $\mathbf{3}^{2+}\cdot 2\mathrm{TfO}^-$ showed the first and the second reduction peak at $E_{red} = -1.10$ and -1.71 V ($\Delta E_{red} = 0.61$ V), respectively, with poor reversibility (Fig. 9). The two phosphonio groups seem to contribute modest stabilization of cation radical $\mathbf{3}^{+\bullet}$ and neutral species **3**. Electron donating character of the mesityl group raised the reduction potential of $\mathbf{3}^{2+}$, as compared with 1,4-bis(diethylphenylphosphonio)-2,3,5,6-tetrafluorobenzene ($E_{red} = -0.83$ and -1.46 V vs. Ag/AgCl, $\Delta E_{red} = 0.63$ V) and 1,4-bis(ethyldiphenylphosphonio)-2,3,5,6-tetrafluorobenzene ($E_{red} = -0.76$ and -1.36 V vs. Ag/AgCl, $\Delta E_{red} = 0.60$ V), reported by Weiss et al.,[7] with almost unchanged difference between the first and the second reduction potentials (0.61 V). The large ΔE_{red} value implies benzene/benzene dianion character of these systems (Scheme 1(b)). The bulkiness of mesityl substituent did not give a significant effect on the stability of reduced species of $\mathbf{3}^{2+}$.

Conclusion

Sterically hindered diphosphines **1**, **4**, and **5**, bis(phosphine oxide) **2** and bis(phosphonium salt) $\mathbf{3}^{2+}$ were synthesized and their congested structure was investigated by ^{1}H, ^{19}F, and ^{31}P NMR spectroscopic studies. In particular ^{19}F NMR spectrum was sensitive to the structural change. The crowded structures of **1**, **2**, and $\mathbf{3}^{2+}$ were further revealed by X-ray crystallography in detail. Oxidation of diphosphines **1**, **4**, and **5** was irreversible in spite of the crowded structure around phosphorus atoms. Introduction of alkyl or aryl substituents in place of fluorine atoms lowered the oxidation potential and improved redox properties, although it was not effective enough to give reversible systems. Further introduction of substituents was necessary in order to accomplish the two-step reversible redox systems such as *para*-phenylenediamines. Dimesitylphosphonio derivative $\mathbf{3}^{2+}$ showed 2-step quasi-reversible reduction. Bulky mesityl group did not significantly contribute to the redox properties of $\mathbf{3}^{2+}$.

Experimental

General. ^{1}H, ^{13}C, ^{19}F, and ^{31}P NMR spectra were measured on a Bruker AC200P or a AM600 spectrometer. ^{1}H and ^{13}C NMR chemical shifts are expressed as δ down-field from external tetramethylsilane. ^{19}F and ^{31}P NMR chemical shifts are expressed as δ down-field from external trichlorofluoromethane and 85% H_3PO_4, respectively. Infrared spectra were collected on a Horiba FT-300 spectrometer. Mass spectra were measured on a Hitachi M-2500S with electron impact (EI) ionization at 70 eV or a JEOL HX-110 with fast atom bombardment (FAB) ionization using *m*-nitrobenzyl alcohol matrix. High resolution mass spectra were measured on a JEOL JMX-SX102 with fast atom bombardment (FAB) ionization, using 2-nitrophenyl octyl ether matrix or a JEOL HX-110 with electron impact (EI) ionization. Melting points were measured on a Yanagimoto MP-J3 apparatus without correction. Microanalyses were performed at the Instrumental Analysis Center of Chemistry, Graduate School of Science, Tohoku University. Flush column chromatography were carried out using compressed air over silica gel (Fuji Silysia, BW-300) unless specified otherwise. Tetrahydrofuran and diethyl ether were distilled from sodium diphenylketyl under argon just prior to use. Cyclic voltammograms were measured on BAS CV50W. Glassy carbon, Pt wire, Ag/0.01 mol L^{-1} $AgNO_3$/0.10 mol L^{-1} *n*-Bu_4NClO_4 CH_3CN were used as a working, a counter, and a reference electrode, respectively. Each degassed solution was measured for diphosphines **1**, **4**, or **5** (ca. 10^{-3} mol L^{-1}) in dichloromethane, or bis(phosphonium salt) $\mathbf{3}^{2+}\cdot 2\mathrm{TfO}^-$ (ca. 10^{-4} mol L^{-1}) in benzonitrile with 0.10 mol L^{-1} *n*-Bu_4NClO_4 as a supporting electrolyte.

Synthesis. Dimesitylphosphine.[11] To a THF solution of the mesityl Grignard reagent, prepared from magnesiun (0.60 g, 24.7 mmol), 2-bromomesitylene (4.0 mL, 26.1 mmol) and THF (16 mL), was added phosphorus trichloride (1.00 mL, 11.4 mmol) at -78 °C. This mixture was gradually warmed up to room temperature. Lithium aluminum hydride (0.50 g, 13.2 mmol) suspended in 8 mL of THF was added to the resultant yellow suspension at 0 °C and the mixture was stirred at room temperature for 1 h. The excess hydride was quenched with ethyl acetate (15 mL) at 0 °C and the mixture was extracted with ether, washed with water and saturated NaCl solution, and dried with anhydrous magnesium sulfate. After removal of the drying agent by filtration and evaporation of the solvents, the residue was chromatographed on silica gel (hexane as eluent) to give dimesitylphosphine (1.05 g, 3.90 mmol) in 34%. Dimesitylphosphine: colorless plates; mp 89 – 92 °C (lit, 97—99 °C).[11] ^{1}H NMR (200 MHz, $CDCl_3$) $\delta = 2.23$ (br. s, 6H, Mes-*p*-Me), 2.25 (br. s, 12H, Mes-*o*-Me), 5.24 (d, $^1J_{PH} = 233$ Hz, 1H, P-H), 6.82 (br. s, 4H, Mes-*m*); ^{31}P NMR (81 MHz, $CDCl_3$) $\delta = -92.4$ (d, $^1J_{PH} = 233$ Hz).

1,4-Bis(dimesitylphosphino)-2,3,5,6-tetrafluorobenzene (1). A hexane solution of butyllithium (0.09 mL, 0.14 mmol) was added to a tetrahydrofuran (2 mL) solution of dimesitylphosphine (38.0 mg, 0.14 mmol) at 0 °C. The resultant yellow-red solution was allowed to react with hexafluorobenzene (15 μL, 0.07 mmol) at 0 °C to give a red solution. After the mixture was stirred for 1 h at room temperature, the solvent was removed by evaporation and the residue was twice recrystallized from chloroform–methanol to give **1** (20.7 mg, 0.03 mmol) in 43% yield.

1: Colorless rods (MeOH–$CHCl_3$), mp 264—265 °C; ^{1}H NMR (200 MHz, $CDCl_3$) $\delta = 2.17$ (s, 24H, Mes-*o*-Me), 2.26 (s, 12H, Mes-*p*-Me), 6.82 (d, $^4J_{PH} = 3.4$ Hz, 8H, Mes-*m*); ^{13}C NMR (150 MHz, $CDCl_3$) $\delta = 20.9$ (s, Mes-*p*-Me), 22.6 (d, $^3J_{PC} = 16.9$ Hz, Mes-*o*-Me), 118.8 (m, Mes_2P–C), 127.6 (d, $^1J_{PC} = 17.7$ Hz, Mes-*ipso*), 130.0 (d, $^3J_{PC} = 4.0$ Hz, Mes-*m*), 138.9 (s, Mes-*p*), 142.8 (d, $^2J_{PC} = 18.2$ Hz, Mes-*o*), 146.8 (dm, $^1J_{FC} = 244.5$ Hz, F–C); ^{31}P NMR (81 MHz, $CDCl_3$) $\delta = -46.3$ (br. t, $^3J_{PF} = 34$ Hz); ^{19}F NMR (188 MHz, $CDCl_3$) $\delta = -131.5$ (br. d, $^3J_{PF} = 34$ Hz); MS(EI, 70 eV) *m/z* (rel intensity) 686 (M^+; 100), 671 (M^+-CH_3; 19), 567 (M^+–Mes; 15). HRMS (70 eV, EI) Found: *m/z* 686.2855. Calcd for $C_{42}H_{44}P_2F_4$: M, 686.2854.

1,4-Bis(dimesitylphosphoryl)-2,3,5,6-tetrafluorobenzene (2). Diphosphine **1** (0.101 g, 0.147 mmol) was dissolved in chloroform–acetone (1/1 in volume) and allowed to react with 30% hydrogen peroxide (6.3 mL, 55.6 mmol) at 0 °C. The resultant colorless suspension was stirred for 1.5 h and extracted with ether. The organic layer was washed with water and saturated NaCl solution and dried over anhydrous magnesium sulfate. After removal of the drying agent by filtration and evaporation of the solvents, the residue was recrystallized from dichloromethane–ethanol to afford **2** containing two molecules of ethanol (56.6 mg, 0.0788 mmol) in 54% yield.

2·2EtOH: Colorless plates (CH_2Cl_2–EtOH), mp > 300°C; ^{1}H NMR (600 MHz, $CDCl_3$) $\delta = 1.23$ (t, $^3J_{HH} = 7.02$ Hz, 6H,

CH_3CH_2OH), 1.83 (br. s, 2H, CH_3CH_2OH), 2.27 (br. s, 36H, Mes-*o*, *p*-Me), 3.71 (q, $^3J_{HH}$ = 7.02 Hz, 4H, CH_3CH_2OH), 6.86 (d, $^4J_{PH}$ = 4.13 Hz, 8H, Mes-*m*); ^{13}C NMR (150 MHz, $CDCl_3$) δ = 18.3 (s, CH_3CH_2OH), 21.0 (s, Mes-*p*-Me), 22.8 (d, $^3J_{PC}$ = 5.0 Hz, Mes-*o*-Me), 58.2 (s, CH_3CH_2OH), 122.0 (ddd, $^1J_{PC}$ = 76.8 Hz, $^2J_{FC}$, $^3J_{FC}$ = 16.7 Hz Mes_2P-C), 127.9 (d, $^1J_{PC}$ = 107.3 Hz, Mes-*ipso*), 131.2 (d, $^3J_{PC}$ = 12.1 Hz, Mes-*m*), 142.2 (d, $^4J_{PC}$ = 2.68 Hz, Mes-*p*), 142.3 (d, $^2J_{PC}$ = 11.2 Hz, Mes-*o*), 146.8 (br., F-C); ^{31}P NMR (81 MHz, $CDCl_3$) δ = 21.8 (s); ^{19}F NMR (188 MHz, $CDCl_3$) δ = −129.8, −129.0 (br.); FAB MS *m/z* (rel intensity) 718 (M^+−2EtOH; 16), 703 (M^+−2EtOH−CH_3; 100), 698 (M^+−2EtOH−F−1; 55), 678 (M^+−2EtOH−2F−2; 31), 663 (M^+−2EtOH−2F−CH_3−2; 22), 658 (M^+−2EtOH−4CH_3; 9), 643 (M^+−2EtOH−5CH_3; 9), 583 (M^+−2EtOH −9CH_3; 11). Found: C, 68.51; H, 6.82%. Calcd for $C_{46}H_{56}F_4O_4P_2$: C, 68.14; H, 6.96%; IR (KBr pellet) ν(OH) 3421 cm^{-1}.

1,4-Bis[(dimesityl)methylphosphonio]-2,3,5,6-tetrafluorobenzene bis(trifluoromethanesulfonate) (3^{2+}·2TfO$^-$). To a refluxing solution of diphosphine **1** (30.3 mg, 0.044 mmol) in chlorobenzene (2.5 mL), methyl trifluoromethanesulfonate (1.40 mL, 12.4 mmol) was added under reflux. The resultant yellow-green solution became a colorless suspension after refluxing for 15 min. The mixture was further stirred for 1 h and the solvent was removed in vacuo. Recrystallization of the residue from acetone–hexane gave 3^{2+}·2TfO$^-$ (30.4 mg, 0.03 mmol) in 68% yield.

3^{2+}·2TfO$^-$: Colorless plates (acetone–hexane), mp > 300°C; ^{1}H NMR (200 MHz, $CDCl_3$) δ = 2.29 (br. s, 24H, Mes-*o*-Me), 2.37 (br. s, 12H, Mes-*p*-Me), 3.12 (br. d, $^2J_{PH}$ = 10.4 Hz, 6H, P–Me), 7.18 (br. d, $^4J_{PH}$ = 4.90 Hz, 8H, Mes-*m*); ^{31}P NMR (81 MHz, $CDCl_3$) δ = 7.2 (s); ^{19}F NMR (188 MHz, $CDCl_3$) δ = −127.4 (m), −126.2 (s), −120.4 (s), −118.1 (m), −78.9 (s, CF_3); FAB MS *m/z* (rel intensity) 866 (M^++1−CF_3SO_3; 100), 716 (M^+−CF_3SO_3−Mes−2CH_3; 10), 597 (M^+−2CF_3SO_3−Mes; 66), 433 (M^+− 2CF_3SO_3−2Mes−3CH_3; 45). Found: C, 54.97; H, 4.88%. Calcd for $C_{46}H_{50}F_{10}O_6P_2S_2$: C, 54.44; H, 4.97%.

2,5-Dibutyl-1,4-bis(dimesitylphosphino)-3,6-difluorobenzene (4). To a THF (7 mL) solution of 1,4-bis(dimesitylphosphino)-2,3,5,6-tetrafluorobenzene (105 mg, 0.15 mmol), hexane solution of butyllithium (0.62 mL, 0.92 mmol) was added at room temperature. The resultant dark purple solution was stirred for 1 h and the solvent was removed in vacuo. The residue was washed with methanol to give **4** (92.9 mg, 0.12 mmol) in 80% yield.

4: Pale yellow powder; mp 222—224 °C; ^{1}H NMR (600 MHz, $CDCl_3$) δ = 0.68 (t, 6H, −$CH_2CH_2CH_2CH_3$), 1.10 (sextet, $^3J_{HH}$ = 7.30 Hz, 4H, −$CH_2CH_2CH_2CH_3$), 1.21 (br. m, 4H, −$CH_2CH_2CH_2CH_3$), 2.12 (s, 24H, Mes-*o*-Me), 2.26 (s, 12H, Mes-*p*-Me), 2.65 (br. t, $^3J_{HH}$ = 8.34 Hz, 4H, −$CH_2CH_2CH_2CH_3$), 6.79 (d, $^4J_{PH}$ = 3.14 Hz, 8H, Mes-*m*); ^{13}C NMR (150 MHz, $CDCl_3$) δ = 13.7 (s, −$CH_2CH_2CH_2CH_3$), 20.9 (s, Mes-*p*-Me), 22.6 (d, $^3J_{PC}$ = 16.5 Hz, Mes-*o*-Me), 22.7 (s, −$CH_2CH_2CH_2CH_3$), 27.7 (d, $^3J_{FC}$ = 26.7 Hz, −$CH_2CH_2CH_2CH_3$), 31.2 (s, −$CH_2CH_2CH_2CH_3$), 126.4 (m, Mes_2P-C), 129.7 (d, $^3J_{PC}$ = 3.6 Hz, Mes-*m*), 130.3 (d, $^1J_{PC}$ = 17.0 Hz, Mes-*ipso*), 132.9 (m, Bu-C), 137.8 (s, Mes-*p*), 142.6 (d, $^2J_{PC}$ = 17.9 Hz, Mes-*o*), 158.8 (ddd, $^1J_{FC}$ = 240.5 Hz, $^2J_{PC}$ = 9.8 Hz, $^3J_{PC}$ = 3.2 Hz, F-C); ^{31}P NMR (81 MHz, $CDCl_3$) δ = −43.6 (br. m); ^{19}F NMR (188 MHz, $CDCl_3$) δ = −106.7 (m); FAB MS *m/z* (rel intensity) 762 (M^+; 97), 705 (M^+−Bu; 17), 643 (M^+−Mes; 27). HRMS (FAB) Found: *m/z* 762.4322. Calcd for $C_{50}H_{62}F_2P_2$: M, 762.4295.

1,4-Bis(dimesitylphosphino)-2,5-difluoro-3,6-diphenylbenzene (5). To a THF (10 mL) solution of 1,4-bis(dimesitylphosphino)-2,3,5,6-tetrafluorobenzene (153 mg, 0.22 mmol), cyclohexane–ether solution of phenyllithium (1.30 mL, 1.34 mmol) was added at room temperature and the resultant dark purple solution was refluxed for 30 min. After the mixture was cooled to room temperature, water (20 mL) and ether (20 mL) was added at 0 °C. The organic layer was washed with brine and dried over anhydrous magnesium sulfate. After removal of the drying agent by filtration and evaporation of the solvents, the residue was purified by flash chromatography over silica gel (hexane, hexane/ether = 1/1) to give **5** (103.4 mg, 0.13 mmol) in 58 % yield. **5**: Yellow powder; mp 246—248 °C; ^{1}H NMR (600 MHz, C_6D_6) δ = 2.01 (s, 12H, Mes-*p*-Me), 2.27 (s, 24H, Mes-*o*-Me), 6.64 (d, $^4J_{PH}$ = 3.16 Hz, 8H, Mes-*m*), 6.91 (m, 6H, Ph-*o*, *p*), 7.11 (m, 4H, Ph-*m*); ^{13}C NMR (150 MHz, C_6D_6) δ = 20.9 (s, Mes-*p*-Me), 22.9 (d, $^3J_{PC}$ = 16.8 Hz, Mes-*o*-Me), 127.7, 127.8 (s, Ph-*m*, *p*), 129.3 (m, Mes_2P-C), 129.8 (d, $^4J_{FC}$ = 3.1 Hz, Ph-*o*), 130.3 (d, $^3J_{PC}$ = 3.6 Hz, Mes-*m*), 131.1 (d, $^1J_{PC}$ = 18.5 Hz, Mes-*ipso*), 135.2 (d, $^3J_{FC}$ = 9.0 Hz, Ph-*ipso*), 136.2 (m, Ph-C), 138.1 (s, Mes-*p*), 142.7 (d, $^2J_{PC}$ = 18.2 Hz, Mes-*o*), 158.2 (ddd, $^1J_{FC}$ = 245.5 Hz, $^2J_{PC}$ = 9.9 Hz, $^3J_{PC}$ = 3.7 Hz, F-C); ^{31}P NMR (81 MHz, C_6D_6) δ = −38.7 (m); ^{19}F NMR (188 MHz, C_6D_6) δ = −100.1 (m); FAB MS *m/z* (rel intensity) 802 (M^+; 100), 683 (M^+−Mes; 56), 563 (M^+−2Mes−1; 23). HRMS (FAB) Found: *m/z* 802.3669. Calcd for $C_{54}H_{54}F_2P_2$: M, 802.3669.

X-Ray Crystallography of 1, 2·2EtOH, and 3^{2+}·2TfO$^-$. All measurements were made on a Rigaku AFC7S diffractometer with graphite monochromated Mo $K\alpha$ radiation (λ = 0.71069 Å. The data were collected at a temperature of 23 °C using the ω–2θ scan technique to a maximum 2θ value of 50.0°. Absorption correction was not applied except for **2**·2EtOH, where an empirical absorption correction based on azimuthal scans of several reflections was applied. Structure solution, refinement, and graphical representation were carried out using teXsan package.[20] Crystallographic data (excluding structure factors) for the structure reported in this paper have been deposited with the Cambridge Data Centre as supplementary publication no. CCDC-113243, 113244, and 113245 for **1**, **2**·2EtOH, and 3^{2+}·2TfO$^-$, respectively. Copies of the data can be obtained free of charge on application to CCDC, 12 Union Road, Cambridge CB2 1EZ, UK (fax: (+44)1223-336-033; e-mail: deposit@ccdc.cam.ac.uk). The complete $F_o - F_c$ data are deposited as Document No. 72005 at the Office of the Editor of Bull. Chem. Soc. Jpn.

Crystal Data for 1. $C_{42}H_{44}F_4P_2$, M = 686.75, colorless prism grown from chloroform–methanol, crystal dimensions 0.50×0.15×0.10 mm^3. Tetragonal, space group $P4/n$ (#85), a = 16.764(2), c = 12.840(3) Å, V = 3608.4(10) Å^3, Z = 4, ρ_{calcd} = 1.264 g cm^{-3}, μ = 0.170 mm^{-1}, $F(000)$ = 1448.00. The number of reflections measured was 3405 ($2\theta_{max}$ = 50.0°), in which 3176 were unique with R_{int} = 0.035, and 1846 were larger than threshold [$I > 2.00\sigma(I)$]. The structure was solved by direct methods (SIR92),[21] expanded using Fourier techniques (DIRDIF94),[22] and refined by full matrix least squares on F^2 for all unique reflections and 306 variable parameters. The non-hydrogen atoms were refined anisotropically. Hydrogen atoms were refined isotropically. R_2 = 0.0684, wR_2 = 0.0624, Goodness of fit S = 1.280 for all. R_1 = 0.0494, wR_1 = 0.0545 for [$I > 2.00\sigma(I)$].

Crystal Data for 2·2EtOH. $C_{46}H_{56}O_4F_4P_2$, M = 810.89, colorless prism grown from dichloromethane–ethanol, crystal dimensions 0.70×0.50×0.25 mm^3. Monoclinic, space group $P2_1/n$ (#14), a = 12.167(4), b = 11.868(3), c = 16.009(3) Å, β = 111.32(1)°, V = 2153.5(8) Å^3, Z = 2, ρ_{calcd} = 1.250 g cm^{-3}, μ = 0.160 mm^{-1}, $F(000)$ = 860.00. The number of reflections measured was 3983 ($2\theta_{max}$ = 50.0°), in which 3793 were unique with R_{int} = 0.041, and 2847 were larger than threshold [$I > 2.00\sigma(I)$]. The structure was

solved by direct methods (SIR92),[21] expanded using Fourier techniques (DIRDIF94),[22] and refined by full matrix least squares on F^2 for all unique reflections and 254 variable parameters. The non-hydrogen atoms were refined anisotropically. Hydrogen atoms were included but not refined. $R_2 = 0.1028$, $wR_2 = 0.1156$, Goodness of fit $S = 7.345$ for all. $R_1 = 0.0866$, $wR_1 = 0.1146$ for $[I > 2.00\sigma(I)]$.

Crystal Data for $3^{2+}\cdot 2TfO^-$. $C_{46}H_{50}O_6F_{10}P_2S_2$, $M = 1014.95$, colorless prism grown from acetone–hexane, crystal dimensions $0.22\times0.15\times0.05$ mm^3. Triclinic, space group $P\bar{1}$ (#2), $a = 13.36(1)$, $b = 16.20(1)$, $c = 12.206(7)$ Å, $\alpha = 105.31(5)°$, $\beta = 102.66(6)°$, $\gamma = 71.74(6)°$, $V = 2394(2)$ Å^3, $Z = 2$, $\rho_{calcd} = 1.408$ g cm^{-3}, $\mu = 0.263$ mm^{-1}, $F(000) = 1052.00$. The numbers of reflections measured was 8746 ($2\theta_{max} = 50.0°$), in which 8423 were unique with $R_{int} = 0.077$, and 2933 were larger than threshold $[I > 2.00\sigma(I)]$. The structure was solved by direct methods (SIR92),[21] expanded using Fourier techniques (DIRDIF94),[22] and refined by full matrix least squares on F^2 for all unique reflections and 595 variable parameters. The non-hydrogen atoms were refined anisotropically. Hydrogen atoms were included but not refined. $R_2 = 0.2122$, $wR_2 = 0.1316$, Goodness of fit $S = 1.1450$ for all. $R_1 = 0.0849$, $wR_1 = 0.1022$ for $[I > 2.00\sigma(I)]$.

The authors are grateful for financial support to The Japan Securities Scholarship Foundation and Grants-in-Aid for Scientific Research from the Ministry of Education, Science, Sports and Culture (Nos. 08454193 and 09239101). Shin-Etsu Chemical Co. is also gratefully appreciated for donation of silicon chemicals. The authors also thank Instrumental Analysis Center for Chemistry, Graduate School of Science, Tohoku University for the measurement of mass spectra and 600 MHz NMR spectra, and for taking elemental analyses.

References

1) S. Sasaki, F. Murakami, and M. Yoshifuji, *Tetrahedron Lett.*, **38**, 7095 (1997).

2) B. I. Stepanov, E. N. Karpova, and A. I. Bokanov, *Zh. Obshch. Khim.*, **39**, 1544 (1968).

3) J. F. Blount, C. A. Maryanoff, and K. Mislow, *Tetrahedron Lett.*, **11**, 913 (1975).

4) J. J. Daly, *J. Chem. Soc.*, **1964**, 3799.

5) a) M. Culcasi, Y. Berchadsky, G. Gronchi, and P. Tordo, *J. Org. Chem.*, **56**, 3537 (1991); b) A. V. Il'yasov, Yu. M. Kargin, and A. A. Vafina, *Russ. J. Gen. Chem.*, **63**, 1833 (1994).

6) S. Dapperheld, E. Steckhan, K.-H. G. Brinkhaus, and T. Esch, *Chem. Ber.*, **124**, 2557 (1991); A. Bewick, D. Serve, and T. A. Joslin, *J. Electrlanal. Chem.*, **154**, 81 (1983); P. Strohriegl and G. Jesberger, *Makromol. Chem.*, **193**, 909 (1992); S. Sasaki and M. Iyoda, *Chem. Lett.*, **1995**, 1011.

7) R. Weiss, R. May, and B. Pomrehn, *Angew. Chem., Int. Ed. Engl.*, **35**, 1232 (1996).

8) R. A. Baldwin and M. T. Cheng, *J. Org. Chem.*, **32**, 1572 (1967).

9) S. E. Tunney and J. K. Stille, *J. Org. Chem.*, **52**, 748 (1987); D. J. Ager, M. B. East, A. Eisenstadt, and S. A. Laneman, *Chem. Commun.*, **1997**, 2359.

10) H. C. E. McFarlane and W. McFarlane, *Polyhedron*, **7**, 1875 (1988); H. C. E. McFarlane and W. McFarlane, *Polyhedron*, **2**, 303 (1988).

11) R. A. Bartlett, M. M. Ormstead, P. P. Power, and G. A. Sigel, *Inorg. Chem.*, **26**, 1941 (1987).

12) Substitution at 1,4-positions: M. Hudlicky, "Chemistry of Organic Fluorine Compounds. A Laboratory Manual with Comprehensive Literature Coverage," 2nd ed, Ellis Horwood Ltd., 1976, p. 380.

13) H. R. Hanna and J. M. Miller, *Can. J. Chem.*, **57**, 1011 (1979).

14) M. Hudlicky, "Chemistry of Organic Fluorine Compounds. A Laboratory Manual with Comprehensive Literature Coverage," 2nd ed., Ellis Horwood Ltd., 1976, p. 579.

15) A. Bayer, G. A. Bowmaker, and H. Schmidbaur, *Inorg. Chem.*, **35**, 5959 (1996).

16) a) G. Bandoli, G. Bortolozzo, D. A. Clemente, U. Croatto, and C. Panattoni, *J. Chem. Soc. A*, **1970**, 2778; b) G. Ruban and V. Zabel, *Cryst. Struct. Commun.*, **6**, 671 (1976); c) A. L. Spek, *Acta Crystallogr., Sect. C*, **C43**, 1233 (1987).

17) a) M. C. Etter, R. D. Gillard, W. B. Gleason, J. K. Rasmussen, R. W. Duerst, and R. B. Johnson, *J. Org. Chem.*, **51**, 5405 (1986); b) C. Lariucci, R. H. de A. Santos, and J. R. Lechat, *Acta Crystallogr., Sect. C*, **C42**, 1825 (1986).

18) M. C. Etter and P. W. Baures, *J. Am. Chem. Soc.*, **110**, 639 (1988).

19) E. Durcankká, I. Ondrejkovicoá, and G. Ondrejovic, *Acta Crystallogr., Sect. C*, **C42**, 1331 (1986).

20) "teXsan; Single Crystal Structure Analysis Software," Version 1.9, Molecular Structure Corporation, Rigaku Corporation (1998).

21) A. Altomare, M. C. Burla, M. Camalli, M. Cascarano, C. Giacovazzo, A. Guagliardi, and G. Polidori, *J. Appl. Crystallogr.*, **27**, 435 (1994).

22) P. T. Beuskens, G. Admiraal, G. Beuskens, W. P. Bosman, R. de Gelder, R. Israel, and J. M. M. Smits. "The DIRDIF-94 Program System, Technical Report of the Crystallography Laboratory," University of Nijmegen, The Netherlands (1994).